Calculations of hyperfine parameters in antimony compounds

A. Svane
Department of Physics and Astronomy, University of Aarhus, DK-8000 Aarhus C, Denmark
(Received 5 May 2003; published 26 August 2003)

The electron contact density and electric-field gradient on the Sb nuclear position is calculated in a series of 22 Sb compounds, comprising metallic, covalent as well as ionic Sb(III) and Sb(V) systems. The full-potential linear-muffin-tin-orbitals method is used with the local-density-approximation for exchange and correlation effects. By comparison with experimental ^{121}Sb and ^{123}Sb nuclear quadrupole resonance data and ^{121}Sb Mössbauer data, the calibration constants relating measured quadrupole coupling constants and isomer shifts to the electric-field gradient and the electron contact density, respectively, are derived. This leads to an accurate determination of the quadrupole moment of the ^{121}Sb nuclear ground state as $Q=-66.9$ fm^2. The difference between the mean-square radius of the ^{121}Sb nucleus in its excited isomeric and ground states is found to be $\Delta\langle r^2\rangle=-0.0521$ fm^2.

DOI: 10.1103/PhysRevB.68.064422 PACS number(s): 76.60.Gv, 76.80.+y, 27.60.+j, 71.20.Ps

I. INTRODUCTION

Nuclear methods, such as nuclear quadrupole resonance[1,2] (NQR) and Mössbauer spectroscopy,[3,4] are widely used for investigations of solid-state systems on an atomic scale. The measured signals depend on parameters of both the particular nuclear isotope employed and the solid-state environment, and to extract reliable information about the latter the former needs to be known with great precision, which constitutes the calibration process of the techniques. The present study considers this calibration for the case of Sb, for which the two naturally abundant isotopes ^{121}Sb and ^{123}Sb are both used in NQR, and the former in addition possesses an isomeric level suitable for Mössbauer spectroscopy.

NQR exploits the resonance of an applied radio frequency field with nuclear transitions between levels created by the interaction between the nuclear quadrupole moment and the electric-field gradient at the nucleus. The nuclear quadrupole moment is an intrinsic property of the nucleus, while the electric-field gradient depends on the chemical environment of the probe nucleus. The Hamiltonian describing the interaction may be written as[1]

$$H=\frac{eV_{zz}Q}{4I(2I-1)}\left\{3\hat{I}_z^2-I(I+1)+\frac{1}{2}\eta(\hat{I}_+^2+\hat{I}_-^2)\right\}. \quad (1)$$

Here, Q is the nuclear quadrupole moment and $\hat{I}=(\hat{I}_x,\hat{I}_y,\hat{I}_z)$ is the nuclear spin with eigenvalue I ($I=5/2$ for ^{121}Sb and $I=7/2$ for ^{123}Sb), and $\hat{I}_+=\hat{I}_x+i\hat{I}_y$ and $\hat{I}_-=\hat{I}_x-i\hat{I}_y$. V_{zz} and η are the electric-field gradient and the asymmetry parameter, respectively, which are given by the nonspherical part ($\ell=2$ component) of the electrostatic potential V from which the second derivative tensor

$$V_{ij}=\frac{\partial V}{\partial x_i\partial x_j}\Big|_{\mathbf{r}=0} \quad (2)$$

is obtained. Denoting the eigenvalues of V_{ij} by V_{xx}, V_{yy}, and V_{zz} with $|V_{xx}|\leqslant|V_{yy}|\leqslant|V_{zz}|$, the electric-field gradient per definition is equal to V_{zz}, while the asymmetry parameter is

$$\eta=\frac{V_{xx}-V_{yy}}{V_{zz}},$$

which lies in the range $[0,1]$ (since $V_{xx}+V_{yy}+V_{zz}=0$). In axial symmetry, $\eta=0$, and the eigenvalues of H are readily obtained:

$$E(m)=\frac{eV_{zz}Q}{4I(2I-1)}\{3m^2-I(I+1)\},$$

where m is the quantum number of $\hat{I}_z$. In the general case, $\eta\neq0$, H must be diagonalized, and the measurement of the level spacing will lead to determination of η. With the prefactor containing the product (the quadrupole coupling constant) $eV_{zz}Q$, the electric-field gradient cannot be directly extracted. In the past, values of Q for ^{121}Sb of $Q=-0.53\pm0.10$ b,[5] $Q=-0.26\pm0.10$ b,[6] $Q=-0.45$ b,[7] and $Q=-0.36$ b (Refs. 8 and 9) have been reported. From NQR measurements of ^{121}Sb and ^{123}Sb in the same compound, an accurate value for the ratio

$$\frac{Q(123)}{Q(121)}=1.2747 \quad (3)$$

is determined.[10] In the present work we will calculate from first principles the electric-field gradient V_{zz} in a number of solids containing Sb, and by comparison to the measured quadrupole coupling constant derive a value of Q, which then can be considered the experimental value of this important parameter of the ^{121}Sb nuclear ground state.

The isomer shift of a nuclear transition energy is given by[4]

$$\delta E_{IS}=\alpha(\rho_a(0)-\rho_s(0)), \quad (4)$$

where $\rho_a(0)$ and $\rho_s(0)$ are the electron charge densities at the nuclear positions (the contact densities) in two different solid-state environments, here denoted the absorber (a) and the source (s) materials, respectively. The electron contact densities carry the information on the solid-state system, while the calibration constant α depends only on the details

of the nuclear transition. In Mössbauer spectroscopy, δE_{IS} is measured as a relative velocity of the absorber and source materials, and α is given by

$$\alpha = \beta \Delta \langle r^2 \rangle, \tag{5}$$

where $\Delta\langle r^2\rangle$ is the difference between the mean-square radius of the Mössbauer nucleus in its excited state and its ground state, and β is a numerical constant [for ^{121}Sb, $\beta = 8.4 a_0^3$ mm/(s fm^2), with a_0 being the Bohr radius].[11] If the simplified picture of a uniform sphere is adopted for the nucleus the calibration constant may be related to the relative change of the nuclear radius as $\alpha = \gamma \Delta R/R$ (with $\gamma = 354.2$ a$_0^3$ mm/s for ^{121}Sb).[11] In this work we will also calculate the electron contact densities in a series of Sb compounds to demonstrate the above linear relationship, Eq. (4), and derive the nuclear parameter $\Delta\langle r^2\rangle$ for ^{121}Sb.

The quadrupole interaction, Eq. (1), leads to a complicated fine structure[12] of the Mössbauer absorption line. For ^{121}Sb both the ground state and the excited isomeric level are split, each with its quadrupole moment, and the natural linewidth of the transition is comparable to the fine structure, leading to an unresolved spectrum. Fitting of the spectra often assumes that η is negligible and that the ratio of the quadrupole moments is given as[13]

$$\frac{Q(121^*)}{Q(121)} = 1.32 \pm 0.01.$$

For these reasons, the extraction of quadrupole coupling constants from Mössbauer experiments is less accurate than NQR (by 2–3 orders of magnitude). However, in contrast to NQR, the asymmetry of the Mössbauer spectrum allows a determination of the sign of the electric-field gradient.

In the present work it will be demonstrated that the NQR and Mössbauer parameters may be calculated with high precision with the full-potential linear-muffin-tin-orbitals (FP-LMTO) method[14] within the local-density approximation (LDA) to density-functional theory.[15] By a comparison to experimental data we will verify the basic linear relations between the quadrupole coupling constants and the electric-field gradient and between the isomer shift and the electron contact density. A wide span of chemical bonding in Sb compounds will be considered, comprising metallic and covalent systems, as well as ionic systems containing both Sb(III) and Sb(V) ions. As a result, *ab initio* calculations may now be considered a part of the spectroscopy, in the sense that such calculations may be used in the interpretation of experimental results.[16,17]

The calibration of Mössbauer experiments has been an issue for a long time.[3,4,18–23] The nuclear parameters, $\Delta\langle r^2\rangle$ and Q are in principle assessible from first-principles nuclear models, but the accuracy of such models is not always good enough to match the accuracy of Mössbauer experiments. More accurate is the determination of nuclear parameters from comparison of calculated electron contact densities[18] or electric-field gradients[19] with corresponding experimental isomer shifts and quadrupole splittings. The isomer shifts of ^{121}Sb have been theoretically investigated previously,[18,24,22,25] and Sb quadrupole coupling constants recently in Refs. 25 and 17.

II. DETAILS OF THE CALCULATIONS

The electronic structures of Sb compounds is calculated with the FP-LMTO method[14] using the LDA for exchange and correlation effects.[15] This method expands the electron wave functions in terms of muffin-tin orbitals,[26] which are atom-centered Neumann functions augmented inside muffin-tin spheres by the numerical solution of the radial scalar-relativistic Dirac equation in the self-consistent crystal potential, together with the energy derivative of this solution.[27] This construction has proven very accurate for solid-state calculations.[28] Three different decay constants for the envelope functions are used. The basis set includes for each atom three orbitals of s character, 3×3 orbitals of p character, 2×5 orbitals of d character, and for Sb 1×7 orbitals of f character. In addition, local orbitals[29] are included to describe semicore states (such as Sb $4p$ and $4d$ states), the polarization of which may contribute significantly to the electric-field gradient and the electron contact density. No shape approximation for the crystal potential is invoked. The crystalline charge density is evaluated exactly within muffin-tin spheres, while in the interstitial region an interpolation scheme is used to obtain the charge density.[14] To increase the accuracy of the interpolation scheme, additional ''empty'' muffin-tin spheres are introduced for crystal structures with open regions of the unit cell. The O $2s$ and F $2s$ states are treated as valence states in the oxides and fluorides. The same methodology has been employed in recent work on interpretation of Mössbauer data of ^{57}Fe,[16] ^{119}Sn,[20] and ^{237}Np.[23]

The FP-LMTO method solves the Schrödinger equation for the electrons in the solid. The electric-field gradient is determined from the electrostatic potential, Eq. (2), which is also the dominant part of the LDA effective potential of the electrons. Hence the V_{ij} tensor is readily obtained and diagonalized. The electron contact density of the Sb nucleus in the Sb compounds is determined by modeling the nucleus as a uniformly charged sphere of radius $R = 1.2A^{1/3}$ fm,[30] where $A = 121$ is the mass number of the Sb Mössbauer nucleus. The contact density is obtained as an average of the electron density over the nuclear volume. At the same time the finite nucleus provides a regularization of the Coulomb potential at the nuclear position. All core states are calculated self-consistently in the crystalline environment. The number of k vectors in the irreducible wedge of the Brillouin zone is chosen such as to obtain a well-converged electric-field gradient and electron contact density.

The compounds considered in this work are listed in Table I. All calculations are performed with the experimental crystal structures, which are given in Ref. 31 and references therein, and Ref. 32.

III. RESULTS

The calculated electric-field gradients and electron contact densities of Sb compounds are listed in Table I together with

TABLE I. Calculated electron contact densities $\rho(0)$ electric-field gradients V_{zz}, and asymmetry parameters η together with experimental nuclear quadrupole coupling constant $\nu_Q = eV_{zz}Q/h$, asymmetry parameter, Mössbauer isomer shifts δE_{IS}, and quadrupole splitting parameter $\Delta = eV_{zz}Q$ for 22 Sb compounds. Units are a_0^{-3} for the electron contact densities, where a large constant ($212\,600 a_0^{-3}$) has been subtracted. The electric-field gradients are in units of 10^{21} V/m^2, the NQR frequency in MHz, and the isomer shifts and quadrupole splittings in units of mm/s.

	Theory			Experiment			
Compound [a]	$\rho(0)$	V_{zz}	η	δE_{IS} [b]	ν_Q [c]	η [c]	Δ [b]
SbF_3	48.65	−32.56	0.15	−14.7	541.30 [d]	0.048 [d]	19.7
$SbCl_3$	46.32	−22.96	0.20	−14.4	383.6	0.188	12.8
$SbCl_5$	22.78	−4.99	0	−3.4	84.67(210 K)	0.0	5.7
$\alpha SbBr_3$	46.82	−18.23	0.19	−14.5	316.02(RT)	0.10	11.6
$\beta SbBr_3$	46.14	−19.02	0.27	−14.5	343.95	0.18	11.6
SbI_3	50.42	−2.62	0	−16.3	84.67	0.003	5.6
Sb_2O_3-cubic	41.47	−34.96	0	−11.4	554.78	0.0	18.3
Sb_2O_3-ortho	42.18	−33.87	0.31	−11.3	541.43	0.36	17.0
Sb_2O_4(III)	48.34	−40.54	0.19	−14.4			16.4
Sb_2O_4(V)	14.67	10.49	0.65	0.67			−6.1
Sb_2O_5	13.44	−6.60	0.91	0.1			−3.7
Sb_2S_3 1	47.33	−14.43	0.40	−14.5	249.76	0.382	7.8
Sb_2S_3 2	47.81	−19.27	0.05	−14.5	317.14	0.014	7.8
Sb_2Se_3 1	47.34	−11.61	0.44	−15.0	198.87	0.417	6.8
Sb_2Se_3 2	46.97	−16.18	0.03	−15.0	272.75	0.008	6.8
Sb_2Te_3	46.94	12.06	0	−15.4			3.8
Sb	39.56	−4.41	0	−11.6	76.85	0.0	0.0
AlSb	29.38	0	0	−7.8	0	0	0
GaSb	31.40	0	0	−8.3	0	0	0
InSb	32.11	0	0	−8.8	0	0	0
SnSb	36.60	0	0	−10.5	0	0	0
MnSb	32.60	4.27	0	−9.1 [e]	73.0 [f](RT)	0.0	0.0
$FeSb_2$	33.75	−22.73	0.56	−10.0 [g]			14.8 [g]
$RuSb_2$	33.19	−24.75	0.67	−9.3 [g]			12.4 [g]
$CoSb_3$	34.76	−15.99	0.68	−9.0 [h]			9.3 [h]

[a]Experimental crystal structures are from Ref. 31 and references therein or Ref. 32.
[b]Experimental Mössbauer data are from Ref. 31 and references therein, except where noted.
[c]Experimental NQR frequencies and η values are from Ref. 2 except where noted. Data refer to low temperature (77 K), except where noted.
[d]Reference 33.
[e]Reference 34.
[f]Reference 35.
[g]Reference 36.
[h]Reference 37.

experimental information on ^{121}Sb NQR frequencies and Mössbauer isomer shifts and quadrupole splittings. All isomer shifts are given relative to a $BaSnO_3$ source and refer to $T=0$. The calculated values are converged to the digits shown, but are of course subject to systematic errors, which are difficult to assess. These include, for example, the validity of the LDA, the scalar relativistic approximation, and other approximations of the calculational scheme, as, e.g., the fitting procedure for the charge density in the interstitial region and restrictions of the basis set employed.

The degree of agreement between experiment and theory may be judged from plots of the experimental versus theoretical values, which are shown in Figs. 1 and 2. In Fig. 1 the experimental isomer shifts are plotted against the calculated electron contact densities. The straight line through the points in Fig. 1 confirms the relationship (4), with the remaining scatter around the line reflecting the combined experimental and theoretical uncertainty. From a best linear fit we derive the calibration constant of Eq. (4):

$$\alpha = (-0.438 \pm 0.013) a_0^{-3} \text{ mm/s} \tag{6}$$

or, using Eq. (5),

$$\Delta\langle r^2\rangle = (-0.0521 \pm 0.0015) \text{ fm}^2. \tag{7}$$

The quoted uncertainties in Eqs. (6) and (7) reflect the scatter of the points around the best straight line, but do not include estimates of systematic errors which may arise from the use

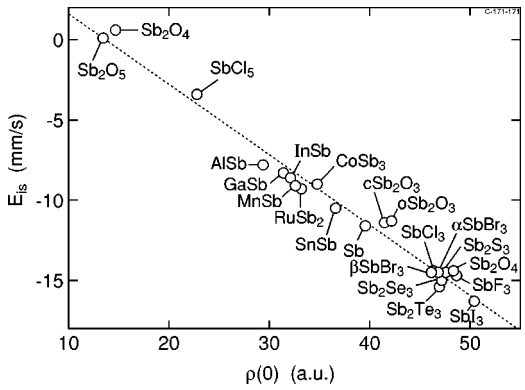

FIG. 1. Calculated electron contact density (in a_0^{-3}) compared to experimental isomer shifts (in mm/s relative to $BaSnO_3$) for Sb compounds. A large constant (212 600 a_0^{-3}) is subtracted from the calculated electron contact density. The dashed line is the best linear fit, Eq. (6).

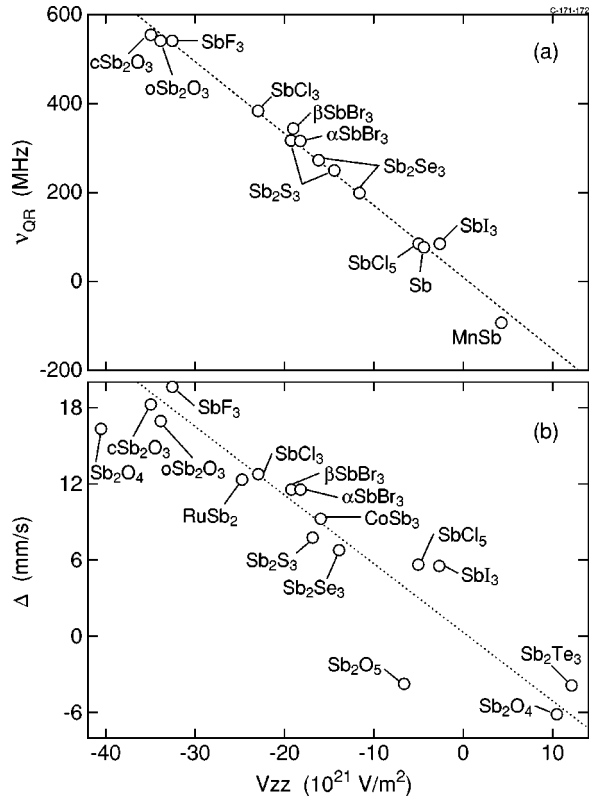

FIG. 2. (a): Calculated electric-field gradient (in units of 10^{21} V/m^2) compared to experimental values for the quadrupole coupling constant $\nu_Q = eV_{zz}Q/h$ as derived from nuclear quadrupole resonance spectroscopy. The latter is expressed in units of MHz. For MnSb the sign of V_{zz} has been changed, since NQR does not reveal the sign of the coupling constant. The dashed line is a best linear fit to the data. (b) Calculated electric-field gradient (in units of 10^{21} V/m^2) compared to experimental values for the quadrupole coupling constant $\Delta = eV_{zz}Q$ as derived from Mössbauer spectroscopy. The latter is expressed in units of mm/s. The dashed line is the best linear fit to the NQR data of (a), which are substantially more accurate than the Mössbauer data. For Sb_2O_5 there is likely to be a sign mismatch between theory and experiment, see text.

of an approximate density functional or a restricted basis set. It is well known that unrelativistic and relativistic charge densities in the vicinity of the nucleus differ largely by a constant factor, which for heavier elements deviates significantly from 1. Similarly, it is conceivable that LDA and full configuration-interaction and basis-set complete charge densities may differ by a factor. To the best of the authors' knowledge, no study has been published addressing this point.

The value Eq. (6), is close to the value derived by Ref. 22, $\alpha = (-0.491 \pm 0.02)\ a_0^{-3}$ mm/s, which also employed the FP-LMTO calculational scheme for the electronic structure of the solid state, albeit in an independent implementation. These authors also showed that the calibration constant does not depend very sensitively on the approximation used to describe exchange and correlation effects (LDA versus generalized gradient approximation). Compared to our previous calibration[24] of ^{121}Sb isomer shifts, the present calibration constant is $\sim$20% larger, but the present work is superior both in employing the much more accurate FP-LMTO method compared to the LMTO-ASA (atomic spheres approximation) method of Ref. 24 and in the incorporation of many more Sb compounds in the analysis.

Figure 2(a) depicts the experimental quadrupole coupling constant versus the calculated electric-field gradient. The linearity is very good and from the best straight line a value of the nuclear quadrupole moment of

$$Q = (-66.9 \pm 1.5)\ \text{fm}^2 \quad \text{for } ^{121}\text{Sb} \tag{8}$$

is derived. The sign of the quadrupole moment does not follow directly from the NQR data, but from Mössbauer data it is clear that it is negative. In plotting Fig. 2 we have associated a negative quadrupole coupling constant with MnSb, since this compound has a positive electric-field gradient. Combined with Eq. (3) this leads to

$$Q = (-85.3 \pm 1.9)\ \text{fm}^2 \quad \text{for} ^{123}\text{Sb}. \tag{9}$$

Again, the uncertainties quoted in Eqs. (8) and (9) merely reflect the statistical fluctuations of the data points in Fig. 2(a), while systematic errors are unknown.

The values for the ^{121}Sb and ^{123}Sb quadrupole moments obtained above are somewhat higher than has been the accepted values hitherto. They are, however, also more precise. In their analysis of quadrupole coupling constants in Sb halide complexes, Poleshchuk *et al.*[25] found the linear relation between the calculated and measured quadrupole coupling constant, but had to scale the experimental values by a factor of 0.69. Unfortunately, these authors do not quote which value they have adopted for the quadrupole moment, but their result is analogous to saying that their value of Q is too small and should be multiplied by a factor of $1/0.69 = 1.45$. Lippens *et al.*[17] have published a figure showing a linear relationship similar to Fig. 2, however, without further analysis. These authors calculated the electric-field gradient using the full-potential linear-augmented-plane-wave (FP-LAPW) method, which is quite similar to the FP-LMTO method em-

ployed here. Estimating the slope of their curve leads to a value of $Q=-64$ fm^2 for ^{121}Sb, in perfect agreement with the present value.

Figure 2(b) shows the quadrupole coupling constant as derived from Mössbauer spectroscopy in comparison with calculated electric-field gradients. These data points show a significantly larger scatter, although they do follow the general linear trends, which then reflects the greater uncertainty of the Mössbauer analysis. For this reason only the NQR data points were included in the linear regression leading to the above value of the nuclear quadrupole moments.

Some of the cases studied contain two crystallographic inequivalent Sb atoms (Sb_2S_3, Sb_2Se_3 and Sb_2O_4). For the first two compounds, the Mössbauer experiments are not able to resolve the spectrums of the two sites. Indeed, the calculations also find very similar electron contact densities in these cases. In the analysis of Fig. 1 we therefore compare the average contact density of the two Sb sites to the experimental isomer shift. The electric-field gradient is different on the two sites, however, and this is also found in NQR. The ratio between the two quadrupole coupling constants measured is 1.27 and 1.37 for Sb_2S_3 and Sb_2Se_3, respectively. The corresponding ratio between calculated electric-field gradients are 1.34 and 1.39, in excellent agreement. Still, these different quadrupole interactions are not resolved in Mössbauer spectroscopy, and in Fig. 2(b) we compare the single quadrupole coupling constants derived from Mössbauer spectra with the average of the calculated field gradients. The Sb_2O_4 compound is peculiar in having Sb atoms in two distinctly different oxidation states, with a markedly different isomer shift, which is readily resolved. This is also revealed in the calculations, which find a difference in contact density between the two Sb atoms of $\sim$33.7 a.u., corresponding to an isomer shift difference of 14.8 mm/s, in perfect agreement with the experimental $\sim$15 mm/s relative shift. In addition, the electric-field gradient of the two sites is rather different, in particular the pentavalent Sb(V) site has a positive field gradient, while the trivalent Sb(III) site has a negative field gradient. The ratio of the two is close to 4, while the ratio of the experimental quadrupole coupling constants is only 2.7, a discrepancy also found in the FP-LAPW calculations and possibly due to an inaccuracy in structure determination.[17] Two systems, Sb_2O_3 and $SbBr_3$, occur in two different crystal structures. In both cases the electric-field gradients and contact densities are rather similar, as revealed both in experiment and in theory.

The electric-field gradient in Sb metal was studied in Ref. 38. The value of $V_{zz}=-4.35\times10^{21}$ V/m^2 is in perfect agreement with ours. Reading off the values of calculated electric-field gradients from the figure of Ref. 17, there seems to be good quantitative agreement with the present values in Table I: $V_{zz}\sim-40$, -36, -35, -24, 0, $+5$, $+10\times10^{21}$ V/m^2, for Sb_2O_4(V), Sb_2O_3, SbF_3, $SbCl_3$, Sb_2Te_3, Sb_2O_5, and Sb_2O_4(III), respectively. Most notable is the disagreement for Sb_2Te_3, for which we have found a positive electric-field gradient of $12.06\cdot10^{21}$ V/m^2, and for Sb_2O_5, for which we find $V_{zz}=-6.60\times10^{21}$ V/m^2, as opposed to the positive value found by Ref. 17, and seemingly confirmed by experiment. The latter compound is a tricky case, though, since the asymmetry parameter is large, $\eta=0.91$, meaning that two components of the electric-field tensor are of almost similar size but different sign. In the limit $\eta=1$ the sign of the electric-field gradient loses its meaning. The experimental report[39] of the experiment for Sb_2O_5 does not quote a value for the asymmetry parameter. Full-potential LMTO calculations of the electric-field gradient and hyperfine fields of MnSb were recently published,[40] however, apparently in the anti-NiAs structure. At least, the published band structure (for MnBi) and total magnetic moments as well as the hyperfine fields and electric-field gradients are in better agreement with those calculated in the present study for the anti-NiAs structure. There is no doubt, though, that MnSb occurs in the anticipated NiAs structure; we find an energy difference of 0.8 eV per formula unit in favor of the NiAs over the anti-NiAs structure. The details of our band-structure calculations are in excellent agreement with that of Ref. 41.

IV. SUMMARY

Electronic structure calculations for a series of Sb compounds comprising all aspects of chemical bonding were presented. The electric-field gradient and electron contact density of Sb nuclei were calculated in the solid-state environment and compared to experimental NQR frequencies and Mössbauer isomer shifts and quadrupole splittings. The expected proportionalities were confirmed. As a consequence accurate values for the ^{121}Sb and ^{123}Sb ground-state quadrupole moments of $Q(121)=-66.9$ fm^2 and $Q(123)=-85.3$ fm^2, respectively, were obtained. For ^{121}Sb the difference in mean-square radius of the nuclear ground-state and excited isomeric state, $\Delta\langle r^2\rangle=-0.0521$ fm^2 was inferred.

ACKNOWLEDGMENT

This work was supported by the Danish Center for Scientific Computing.

[1] T.P. Das and E.L. Hahn, Solid State Phys., Adv. Res. Appl., Suppl. **1**, 1 (1958).
[2] G.K. Semin, T.A. Babushkina, and G.G. Yakobson, *Nuclear Quadrupole Resonance in Chemistry* (Wiley, New York, 1975).
[3] N.N. Greenwood and T.C. Gibb, *Mössbauer Spectroscopy* (Chapman and Hall, London, 1971).
[4] *Mössbauer Isomer Shifts*, edited by G.K. Shenoy and F.E. Wagner (North-Holland, Amsterdam, 1978).
[5] K. Murakawa, Phys. Rev. **100**, 1369 (1955).
[6] S.L. Ruby, G.M. Kalvius, G.B. Beard, and R.E. Snyder, Phys. Rev. **159**, 239 (1967).
[7] J. Dembczynski, Acta Phys. Pol. A **49**, 541 (1976).
[8] B. Buchholz, H.-D. Kronfeldt, G. Müller, M. Voss, and R. Winkler, Z. Phys. A **288**, 247 (1978).

[9] *Table of the Isotopes*, edited by R.B. Firestone and V.S. Shirley, 8th ed. (Wiley, New York, 1996).
[10] T.-C. Wang, Phys. Rev. **99**, 566 (1955).
[11] G.K. Shenoy and B.D. Dunlap, in *Mössbauer Isomer Shifts* (Ref. 4) App. IV.
[12] G.K. Shenoy and B.D. Dunlap, Nucl. Instrum. Methods **71**, 285 (1969).
[13] J.G. Stevens and S.L. Ruby, Phys. Lett. **32A**, 91 (1970).
[14] M. Methfessel, Phys. Rev. B **38**, 1537 (1988); M. Methfessel, C.O. Rodriguez, and O.K. Andersen, *ibid.* **40**, 2009 (1989).
[15] R.O. Jones and O. Gunnarsson, Rev. Mod. Phys. **61**, 689 (1989); we use the parametrization of S.H. Vosko, L. Wilk, and M. Nusair, Can. J. Phys. **58**, 1200 (1980).
[16] M. Fanciulli, A. Zenkevich, I. Wenneker, A. Svane, N.E. Christensen, and G. Weyer, Phys. Rev. B **54**, 15 985 (1996); M. Fanciulli, C. Rosenblad, G. Weyer, A. Svane, N.E. Christensen, and H. von Känel, J. Phys.: Condens. Matter **9**, 1619 (1997); M. Fanciulli, G. Weyer, A. Svane, N.E. Christensen, H. von Känel, E. Müller, N. Onda, L. Miglio, F. Tavazza, and M. Celino, Phys. Rev. B **59**, 3675 (1999); M. Corti, A. Gabetta, M. Fanciulli, A. Svane, and N.E. Christensen, *ibid.* **67**, 064416 (2003).
[17] P.E. Lippens, J.C. Jumas, and J. Olivier-Fourcade, Hyperfine Interact. **141/142**, 303 (2002).
[18] A. Svane and E. Antoncik, Phys. Rev. B **34**, 1944 (1986).
[19] P. Dufek, P. Blaha, and K. Schwarz, Phys. Rev. Lett. **75**, 3545 (1995).
[20] A. Svane, N.E. Christensen, C.O. Rodriguez, and M. Methfessel, Phys. Rev. B **55**, 12 572 (1997).
[21] P.E. Lippens, Phys. Rev. B **60**, 4576 (1999); P.E. Lippens, J. Olivier-Fourcade, and J.C. Jumas, Hyperfine Interact. **126**, 137 (2000).
[22] S. Sharma, J.K. Dewhurst, L. Nordström, and B. Johansson, J. Phys.: Condens. Matter **14**, 3537 (2002).
[23] A. Svane, L. Petit, W.M. Temmerman, and Z. Szotek, Phys. Rev. B **66**, 085110 (2002).
[24] A. Svane and E. Antoncik, J. Phys. C **20**, 2683 (1987).
[25] O.Kh. Poleshchuk, J.N. Latosińska, and V.G. Yakimiv, Phys. Chem. Chem. Phys. **2**, 1877 (2000)
[26] O.K. Andersen, Phys. Rev. B **12**, 3060 (1975).
[27] H.L. Skriver, *The LMTO Method* (Springer Verlag, Berlin, 1984).
[28] O.K. Andersen, O. Jepsen, and O. Glötzel, in *Canonical Description of the Band Structures of Metals*, Proceedings of International School of Physics "Enrico Fermi," Course LXXXIX, Varenna, 1985, edited by F. Bassani, F. Fumi, and M. P. Tosi (North-Holland, Amsterdam, 1985), p. 59.
[29] D.J. Singh, *Planewaves, Pseudopotentials and the LAPW method* (Kluwer, Boston, 1994)
[30] A.J. Freeman and D.E. Ellis, in *Mössbauer Isomer Shifts* (Ref. 4), Chap. 4.
[31] P.E. Lippens, Solid State Commun. **113**, 399 (2000).
[32] P. Villars and L.D. Calvert, *Pearson's Handbook of Crystallographic Data for Intermetallic Phases*, 2nd ed. (ASM International, Ohio, 1991).
[33] V.N. Rykovanov, R.Sh. Lotfullin, L.A. Zemnukhova, A.A. Boguslavskii, and R.L. Davidovich, Phys. Status Solidi B **167**, K51 (1991).
[34] *Antimony 121: References and Data*, edited by J.G. Stevens, R.M. White, J.L. Gibson, P.C. Newman, and D.J. Parker (Mössbauer Effect Data Center, Asheville, 1985).
[35] A. Tsujimora, T. Hihara, and Y. K$\bar{o}$i, J. Phys. Soc. Jpn. **17**, 1078 (1962).
[36] J.D. Donaldson, A. Kjekshus, D.G. Nicholson, and M.J. Tricker, Acta Chem. Scand. (1947-1973) **26**, 3215 (1972).
[37] I. Lefebvre-Devos, M. Lassalle, X. Wallart, J. Olivier-Fourcade, L. Monconduit, and J.C. Jumas, Phys. Rev. B **63**, 125110 (2001).
[38] G.J. Hill, J.M. Keartland, M.J.R. Hoch, and H. Haas, Phys. Rev. B **58**, 13 614 (1998).
[39] M. Jansen, J. Pebler, and K. Dehnicke, Z. Anorg. Allg. Chem. **495**, 120 (1982).
[40] P. Ravindran, A. Delin, P. James, B. Johansson, J.M. Wills, R. Ahuja, and O. Eriksson, Phys. Rev. B **59**, 15 680 (1999).
[41] R. Coehoorn, C. Haas, and R.A. de Groot, Phys. Rev. B **31**, 1980 (1985).